Temperature-Programmed Desorption Study of the Selective Oxidation of Alcohols on Silica-Supported Vanadium Oxide†

T. Feng and J. M. Vohs*

Department of Chemical and Biomolecular Engineering, University of Pennsylvania, Philadelphia, Pennsylvania 19104-6393

Received: February 25, 2004

The partial oxidation of methanol and ethanol on silica-supported vanadium oxide catalysts was studied using temperature-programmed desorption (TPD), Raman spectroscopy, and diffuse reflectance infrared spectroscopy (DRIFTS). Methanol TPD results for V_2O_5/SiO_2 samples as a function of vanadia loading in conjunction with X-ray diffraction data and Raman spectra indicated that dispersed vanadia on silica agglomerates into vanadia crystallites during a CH_3OH TPD experiment. For ethanol-dosed samples, agglomeration of the dispersed vanadia was less severe, and it was possible to measure the activation energy for the dehydrogenation of adsorbed ethoxides to produce CH_3CHO. Assuming a preexponential factor of 10^{13} s^{-1}, the activation energy for this reaction was estimated to be 132 kJ/mol. The results of this study further demonstrate that there is a relatively weak interaction between vanadia and silica and suggest that adsorbed methoxide species help facilitate agglomeration of dispersed vanadia.

Introduction

Vanadia supported on a second oxide is a well-known selective oxidation catalyst that exhibits high activity for the oxidation of *o*-xylene to phthalic anhydride and methanol to formaldehyde.[1−3] Numerous studies have shown that the active form of vanadia in these catalysts consists of monolayer or submonolayer species on the support.[4−8] In contrast to the monolayer phase, bulk vanadia has low activity for selective oxidation reactions. Supported vanadia catalysts have been the subject of numerous investigations, and much is known about the relationships between their structure and reactivity.[9−20] One intriguing aspect of these catalysts that is not completely understood is how the underlying oxide support affects the reactivity of the vanadia layer. While the structure of vanadia monolayers is largely invariant on a wide range of oxide supports,[6,7,21] the activity of the vanadia, for example, as measured by the turnover frequency for the oxidation of methanol to formaldehyde, is strongly influenced by the support and varies by several orders of magnitude.[3,22]

In an effort to provide additional insight into how vanadia-support interactions influence the reactivity, stability, and reducibility of supported vanadia catalysts, we have been using temperature-programmed desorption (TPD) of alcohols in conjunction with spectroscopic probes such as XPS to study this system.[23−30] TPD has proven to be particularly useful because it allows one to directly measure the activation energy of the rate-limiting step for alcohol oxidation. This is in contrast to steady-state kinetics measurements from which only apparent activation energies can be obtained, and these generally contain contributions from not only the activation energy of the rate-limiting step but also the heat of adsorption of the alcohol and the heat of reoxidation of the vanadia layer.[31−33] In our TPD studies, we have used both high surface area vanadia/titania and vanadia/ceria catalysts[25,34] and model catalysts consisting of vapor-deposited vanadia films supported on TiO_2 and CeO_2 single crystals.[23,24,26−28] One interesting result from these studies is the demonstration that the activation energy for the oxidation of adsorbed methoxide species to produce formaldehyde is dependent on the oxidation state of the vanadia in the supported layer. For example, on vanadia/ceria, this reaction occurs near 520 K during methanol TPD on oxidized vanadia monolayers that contain predominantly V^{+5}, while on samples that contain V^{+4} and V^{+3} formaldehyde is produced at 550 and 610 K, respectively. A similar trend has also been observed for vanadia/titania. Thus, the temperature at which CH_2O is produced during CH_3OH TPD can be used as a chemical probe of the oxidation state of the vanadia in the supported layer.

Silica is an interesting support for vanadia and somewhat distinct from the other commonly used oxide supports such as TiO_2, CeO_2, ZrO_2, and Al_2O_3. For very low weight loadings, the structure of vanadia on silica is similar to that on the other oxides and consists of isolated VO_4 species that exhibit a characteristic peak in Raman spectra between 1030 and 1040 cm^{-1}.[6−8,10,12,35−39] In contrast to other oxide supports, the formation of vanadium crystallites on silica occurs well below monolayer coverage, and two-dimensional polyvanadate species are not readily formed.[7,14,15,40] The reactivity of dispersed vanadia on silica is also substantially less than that for vanadia on other supports. For example, Deo and Wachs have reported that the turnover frequency for methanol oxidation on V_2O_5/SiO_2 is over 2 orders of magnitude less than that on V_2O_5/ZrO_2 and V_2O_5/TiO_2.[3,22] To study the origins of the low reactivity for silica-supported vanadia, in this paper we have extended our previous alcohol TPD studies of supported vanadia catalysts to include vanadia supported on silica. Raman, diffuse reflectance Fourier transform infrared spectroscopy (DRIFTS), and X-ray diffraction (XRD) results are also presented.

Experimental Section

Samples consisting of 1, 12, and 20 wt % V_2O_5 supported on SiO_2 (Sigma, S-5005, 400 m^2/g) were prepared by impregna-

† Part of the special issue "Michel Boudart Festschrift".

* Corresponding author. E-mail: vohs@seas.upenn.edu.

10.1021/jp040165k CCC: $30.25
Published on Web 08/04/2004

tion of an aqueous solution of ammonium metavanadate (NH_4VO_3) and oxalic acid ($C_2O_4H_2$, Aldrich) in a 1:2 molar ratio. Following impregnation, each catalyst was dried overnight at 400 K and then calcined in air at 775 K for 5 h. Bulk V_2O_5 (99.99%) was also used in this study and obtained from Aldrich and had a surface area, as determined by the BET method, of 18 m^2/g.

The catalyst structure was characterized using both X-ray diffraction and Raman spectroscopy. Powder X-ray diffraction patterns for $10° \leq 2\theta \leq 70°$ were collected using a Rigaku Dmax diffractometer with Cu Kα X-rays. Raman experiments were performed in the Nanomaterials Laboratory at Drexel University using a Renishaw 1000 Raman spectrometer equipped with an Ar ion laser (514.5 nm) and a CCD detector. All Raman spectra were collected with the samples exposed to ambient air using a laser power of 25 mW. This laser power was sufficiently low to ensure that heating of the sample during data collection was not significant. Forty scans (60 s/scan) were averaged for each Raman spectrum. Previous studies have shown that for these conditions the supported vanadia catalysts are generally hydroxylated, and this can influence the structure of the supported vanadia layer.[8] One, therefore, needs to be careful when using Raman spectra collected under ambient conditions to infer structures that may be present under reaction conditions. Jehng et al. have shown, however, that due to the hydrophobic nature of silica, the structure of vanadia layers on this support is not significantly affected by the introduction of water vapor.[41] Thus, in the case of vanadia on silica, Raman spectra collected at ambient conditions provide at least qualitative insight into the structure of the vanadia deposits that are likely to be present under reaction conditions.

TPD data were collected using a high vacuum apparatus that has previously been described in detail,[34] which consisted of a Cahn vacuum microbalance that was modified to allow the sample to be heated using an external oven. The system was diffusion pumped and equipped with a mass spectrometer (Thermo ONIX). For TPD studies, 30−40 mg of catalyst was loaded into the sample pan of the microbalance, and the system was evacuated to a baseline pressure of 10^{-7} Torr. After being placed into the TPD system, the vanadia/silica sample was pretreated by heating in a vacuum to 475 K to remove adsorbed water, surface hydroxyls, and other weakly adsorbed impurities. For a TPD experiment, the catalyst was initially exposed to ∼15 Torr of methanol or ethanol vapor at room temperature. The exposure time varied somewhat from run to run but was always long enough to ensure that the sample was saturated with the alcohol as determined by a leveling off of the weight gain. After pumping the system back to its base pressure and allowing the sample weight to stabilize, the sample was heated to 800 K at a rate of 15 K/min. While heating, the desorbing species were monitored using the mass spectrometer. Multiple *m*/*e* ratios were collected during each TPD run, and individual products were identified by their characteristic mass fragmentation patterns. The desorption spectra for specific molecules presented below have been corrected for overlapping cracking fragments from other products and quantified using standard procedures.

Diffuse reflectance Fourier transform infrared spectroscopy was used to characterize species adsorbed on the vanadia/silica catalysts. The DRIFTS spectra were collected using an ATI Mattson Galaxy FTIR spectrometer equipped with a Spectra-Tech diffuse-reflectance cell. The sample cell allowed for in situ heating and exposure to controlled gas environments. The DRIFTS spectra were collected at a resolution of 2 cm^{-1}, and 256 scans were averaged for each spectrum. Samples used for the DRIFTS experiments were pretreated in the diffuse-reflectance cell by exposure to flowing O_2 at 475 K for 10 min. This treatment was found to be sufficient to remove adsorbed water and other weakly adsorbed impurities. Samples were exposed to methanol by flowing 13% methanol vapor in helium through the sample cell for 10 min with the sample held at room temperature. Following exposure to the methanol, the DRIFTS cell was purged with He and heated to the desired temperature at which point a spectrum was collected.

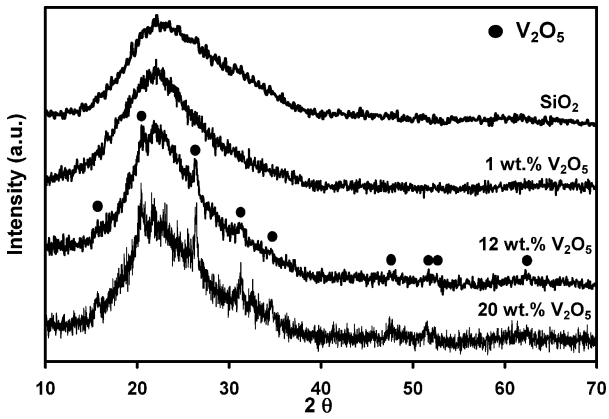

Figure 1. X-ray diffraction patterns of pure SiO_2 and 1, 12, and 20 wt % V_2O_5/SiO_2.

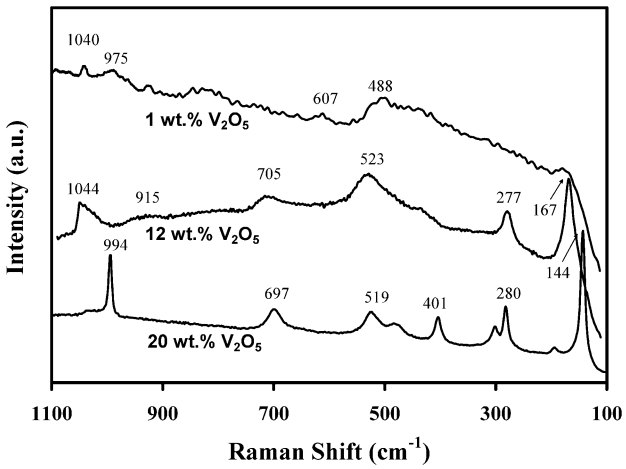

Figure 2. Raman spectra of the 1, 12, and 20 wt % V_2O_5/SiO_2 samples.

Results

X-ray diffraction and Raman spectroscopy were used to characterize the structure of the supported vanadia catalysts used in this study. XRD patterns and Raman spectra of the 1, 12, and 20 wt % V_2O_5/SiO_2 samples are presented in Figures 1 and 2, respectively. As denoted in Figure 1, the XRD patterns for the 12 and 20 wt % V_2O_5/SiO_2 samples contain peaks at 2θ values that are indicative of bulk V_2O_5. Thus, V_2O_5 crystallites are present in these samples. The XRD pattern for the 1 wt % V_2O_5/SiO_2 sample is similar to that of the amorphous silica support and does not contain any discernible peaks due to vanadia.

The Raman spectrum of the 1 wt % V_2O_5 sample (Figure 2) contains numerous peaks which can be assigned on the basis of comparisons to previous studies as follows: the band at 975 cm^{-1} is due to the Si−OH stretching mode of isolated surface hydroxyl groups, the two bands at 607 and 488 cm^{-1} can be attributed to tri- and tetrasiloxane rings, respectively, and the broad features between 400 and 470 cm^{-1} and 750 and 850 are

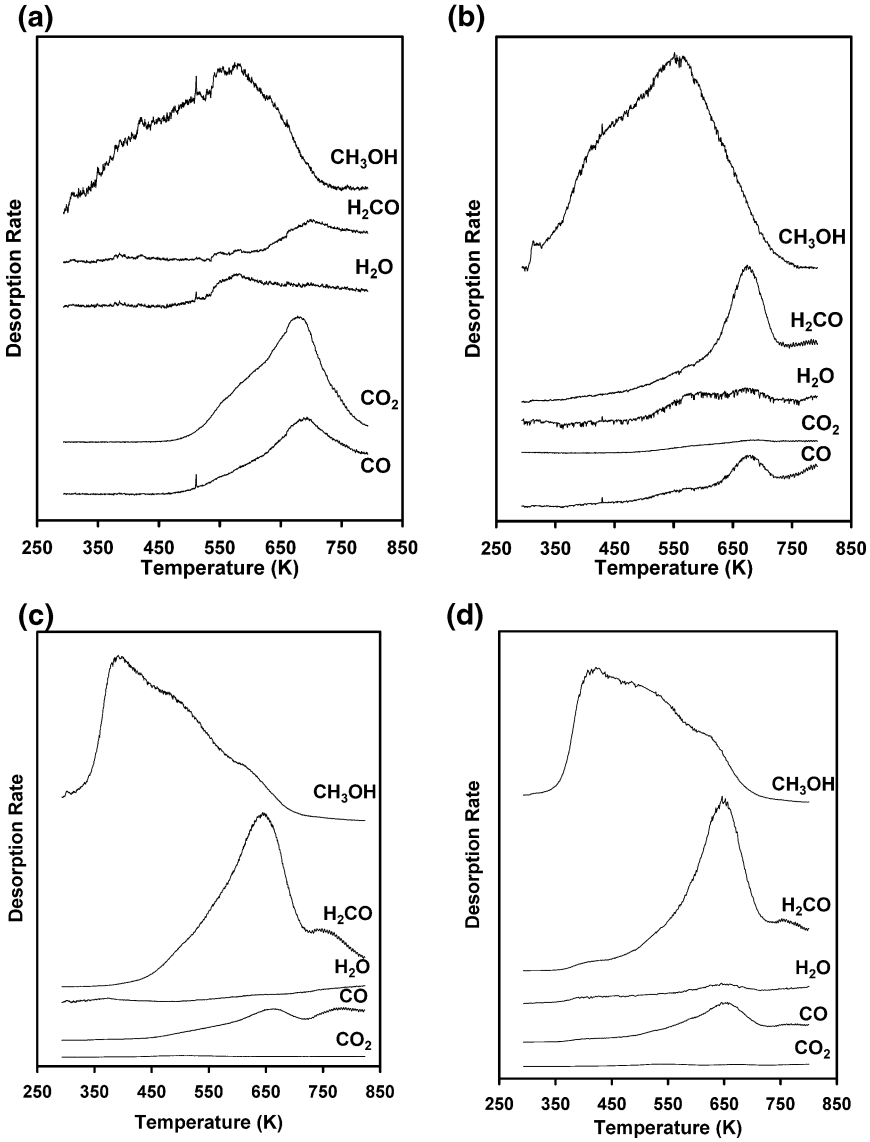

Figure 3. TPD spectra obtained from CH_3OH-dosed (a) bulk V_2O_5, (b) 1 wt % V_2O_5/SiO_2, (c) 12 wt % V_2O_5/SiO_2, and (d) 20 wt % V_2O_5/SiO_2.

due to the symmetric Si−O−Si stretching and Si−O−Si bending modes of the silica support.[13,17,42,43] The peak at 1040 cm^{-1} is characteristic of the V═O stretching vibration of isolated VO_4 species[6,13] and is indicative of highly dispersed vanadia. The Raman spectrum of the 12 wt % vanadia sample also contains a peak at 1044 cm^{-1}, indicating the presence of dispersed VO_4 species. The Raman spectrum of the 20 wt % sample is significantly different than that of the lower coverage samples. The peak at 1040 cm^{-1} due to dispersed monolayer vanadia is nearly absent for this sample, and new peaks at 994, 697, 519, 401, 280, and 144 cm^{-1} have emerged which are indicative of crystalline V_2O_5.[14−16] Together the Raman and XRD data indicate that the 1 wt % V_2O_5/SiO_2 catalyst contained primarily isolated VO_4 species while the 12 wt % sample contained a mixture of both dispersed VO_4 monolayer species and vanadia crystallites and the 20 wt % sample contained primarily V_2O_5 crystallites.

The reactivities of the supported vanadia catalysts toward alcohols were characterized using TPD. For comparison purposes TPD data for the interaction of alcohols with pure silica and vanadia samples were also collected. The only gaseous product detected during TPD from CH_3OH-dosed SiO_2 was CH_3OH, which desorbed in a broad feature which spanned from 350 to 700 K. Previous FTIR studies of the adsorption and reaction of CH_3OH on SiO_2 have demonstrated that CH_3OH adsorbs dissociatively, forming highly stable methoxide species that decompose at temperatures in excess of 900 K.[44] The TPD apparatus used in the present investigation was only able to heat samples to ∼800 K; thus it was not possible to observe the methoxide decomposition reaction. The DRIFTS results presented below show, however, that methoxide species were also formed on the silica sample used in this study. Thus, the results obtained here are in agreement with those reported previously.

Methanol TPD results for pure V_2O_5 are presented in Figure 3a and show, as would be expected, that bulk vanadia is not active for the oxidation of methanol to formaldehyde. The primary oxidation products in the TPD spectra are CO and CO_2, which are produced in broad peaks centered at 675 K. Only a very small amount of CH_2O is produced at 700 K.

Methanol TPD results for the V_2O_5/SiO_2 catalysts are presented in Figure 3b−d. The TPD spectra are similar for all three vanadia weight loadings. Molecular methanol desorbs between 350 and 700 K, and the only oxidation products are CH_2O, CO, and H_2O. For comparison purposes, the CH_2O desorption curve for each sample including bulk vanadia is presented Figure 4. This figure shows that the CH_2O desorption

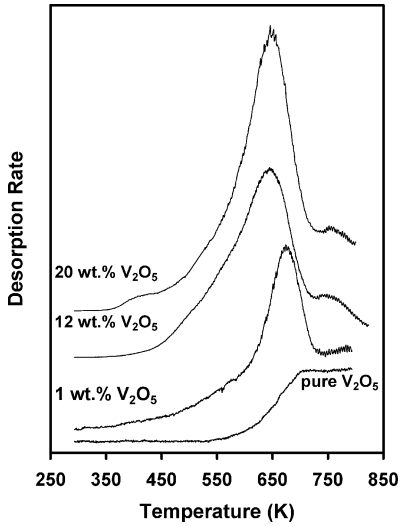

Figure 4. CH_2O desorption spectra obtained during TPD with CH_3OH-dosed pure V_2O_5 and 1, 12, and 20 wt % V_2O_5/SiO_2.

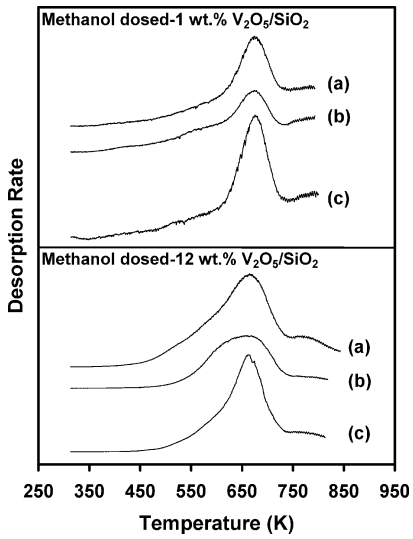

Figure 5. CH_2O desorption spectra obtained from CH_3OH-dosed, 1 and 12 wt % V_2O_5/SiO_2 following various sample pretreatments: (a) freshly prepared sample, (b) subsequent TPD run with the sample used in (a), and (c) after reoxidation of the sample used in (b) in 1 Torr O_2 at 775 K.

spectra are similar for the 12 and 20 wt % samples and contain broad peaks centered at 650 K, and a smaller CH_2O peak is also evident at 760 K. The CH_2O desorption peak for the 1 wt % sample is sharper and at a slightly higher temperature, 675 K, than the primary CH_2O peaks from the higher weight loading samples. All three V_2O_5/SiO_2 samples were selective for the oxidation of CH_3OH to CH_2O, and only small amounts of CO were produced concurrently with the CH_2O.

Figure 5 displays the CH_2O desorption curves obtained during CH_3OH TPD for both the 1 and the 12 wt % V_2O_5/SiO_2 samples as a function of sample pretreatment. In this figure, curve a corresponds to a freshly prepared sample, curve b was obtained in the subsequent CH_3OH TPD run, and curve c was obtained after oxidizing the sample used in (b) in 1 Torr O_2 at 775 K. For both weight loadings, the primary CH_2O desorption peak is centered at 675 K and, with the exception of a reduction in intensity for the sample that had been subjected to a previous TPD run, the pretreatment conditions did not significantly affect the TPD results. This result is in sharp contrast to what was obtained in our previous TPD studies of the reaction of CH_3OH on V_2O_5/TiO_2 and V_2O_5/CeO_2, in which it was found that a CH_3OH TPD run resulted in reduction of the vanadia layer and this caused an increase in the CH_2O peak temperature in the subsequent CH_3OH TPD run. Comparison to these previous TPD studies also reveals that the CH_2O peak temperature for V_2O_5/SiO_2 is substantially higher than that obtained from fully oxidized V_2O_5/TiO_2 and V_2O_5/CeO_2 where the peak was located at 525 K.[25,34] The CH_2O peak temperature for V_2O_5/SiO_2 is even higher than that obtained from reduced V_2O_5/TiO_2 and V_2O_5/CeO_2, which contained vanadium cations primarily in the +3 oxidation state for which CH_2O was produced near 610 K. It is tempting to conclude from these TPD results that the activation energy for the dehydrogenation of methoxide species on dispersed vanadia supported on SiO_2 is significantly higher than that on TiO_2 and CeO_2. While this conclusion would be consistent with the reactivity trends for supported vanadia catalysts reported in the literature, it is somewhat at odds with the TPD data obtained from the 20 wt % V_2O_5/SiO_2 sample. The formaldehyde peak temperature and hence the activation energy for the dehydrogenation reaction on the 20 wt % sample that contained predominantly vanadia crystallites are the same as those obtained for the 12 wt % sample and slightly less than those on the 1 wt % sample, both of which contained dispersed vanadia. One possible explanation for this result is that agglomeration of the dispersed vanadia occurred during the TPD experiment. Thus, CH_2O peaks for the 1 and 12 wt % V_2O_5/SiO_2 samples may also be due to reaction on vanadia crystallites.

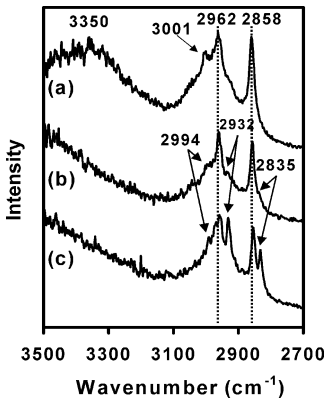

Figure 6. DRIFT spectra obtained after exposure of (a) pure SiO_2, (b) 1 wt % V_2O_5/SiO_2, and (b) 12 wt % V_2O_5/SiO_2 to CH_3OH at 375 K.

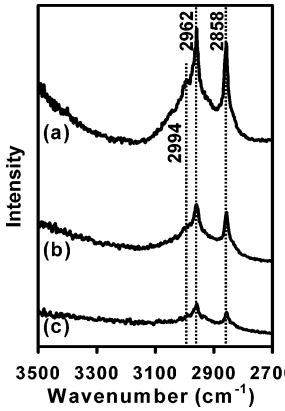

Figure 7. DRIFT spectra obtained after heating CH_3OH-dosed (a) pure SiO_2, (b) 1 wt % V_2O_5/SiO_2, and (c) 12 wt % V_2O_5/SiO_2 to 675 K.

DRIFTS was also used to characterize the interaction of methanol with the 1 and 12 wt % samples. DRIFT spectra for these catalysts obtained following exposure to CH_3OH at 375

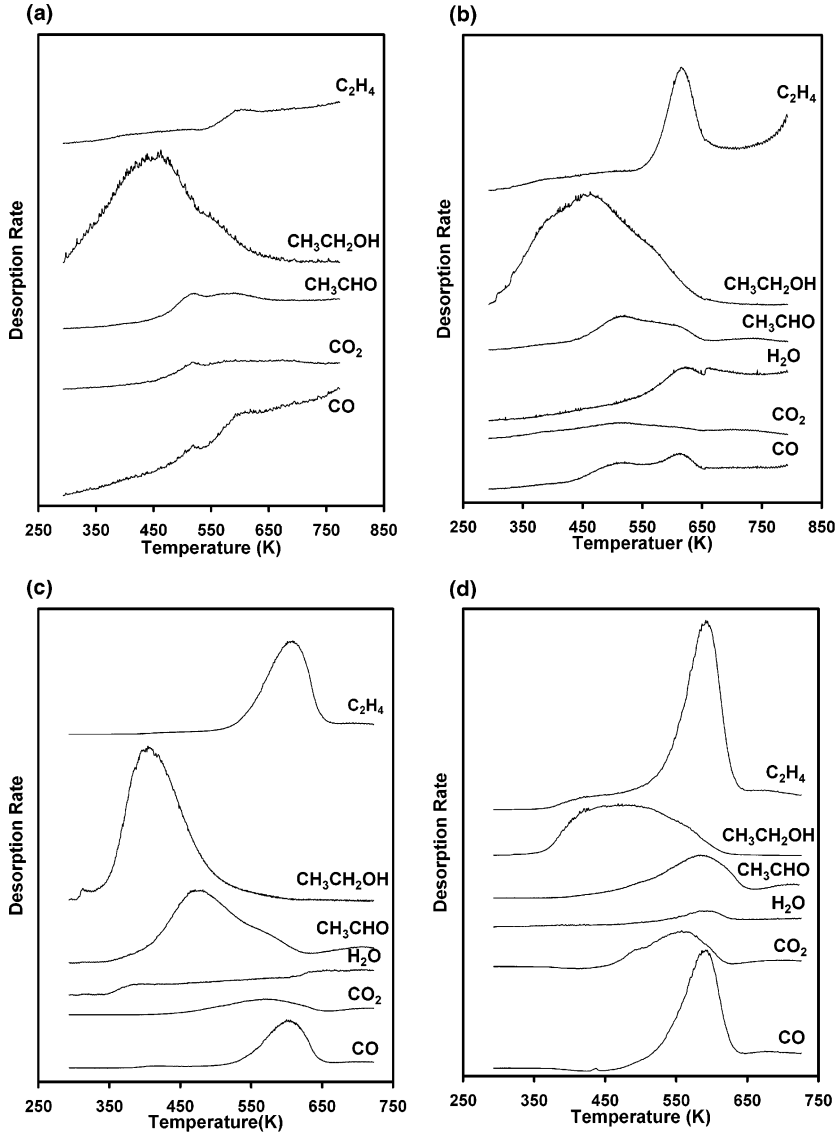

Figure 8. TPD spectra obtained from CH_3CH_2OH-dosed (a) bulk V_2O_5, (b) 1 wt % V_2O_5/SiO_2, (c) 12 wt % V_2O_5/SiO_2, and (d) 20 wt % V_2O_5/SiO_2.

K and heating to 675 K are displayed in Figures 6 and 7, respectively. For comparison purposes, the spectrum of a pure silica sample (curve a) is also included in each figure. The spectrum of the CH_3OH-dosed SiO_2 sample is similar at both 375 and 675 K and contains three peaks in the C−H stretching region at 2858, 2962, and 3001 cm^{-1}, which can be assigned to $\nu_s(CH_3)$, $\nu''_{as}(CH_3)$, and $\nu'_{as}(CH_3)$ modes, respectively, of adsorbed methoxide species.[44−47,49,50] The spectrum obtained at 375 K also contains a broad feature centered at 3350 cm^{-1} which can be attributed to an O−H stretching mode of physisorbed methanol and surface hydroxyl groups.[51] These results are consistent with previous studies[44,49] and demonstrate that both molecular methanol and methoxide species are present on the silica sample at 375 K and primarily the methoxide species remain at 675 K.

The DRIFTS spectra of the CH_3OH-dosed 1 and 12 wt % V_2O_5/SiO_2 samples at 375 K (curves b and c, Figure 6) also contain peaks centered at 2858, 2962, and 2994 cm^{-1} which can be attributed to the C−H stretching modes of methoxide species absorbed on the silica support. These spectra, however, contain two additional peaks centered at 2932 and 2835 cm^{-1}. These peaks increase in intensity with increased vanadia loading and disappear upon heating to 675 K (see curves b and c in Figure 7), demonstrating that they are due to the $\nu(CH_3)$ modes of methoxide species adsorbed on the vanadia. This assignment is also consistent with previous studies.[32,52]

To further investigate the oxidation of alcohols on vanadia/silica, ethanol TPD experiments were also carried out. These TPD results along with those for bulk vanadia are presented in Figure 8. As was the case for methanol, the bulk V_2O_5 sample (Figure 8a) was not highly active for ethanol oxidation, and the primary feature in the TPD spectra is a broad C_2H_5OH desorption peak spanning from 300 to 600 K. Small peaks for C_2H_4, CO, and CO_2 were also observed. The C_2H_5OH TPD spectra for the V_2O_5/SiO_2 samples are more complex than those obtained for CH_3OH and exhibit a stronger dependence on the vanadia weight loading. For the 1 wt % sample (Figure 8b), acetaldehyde was produced in two overlapping peaks centered at 510 and 610 K, CO and a small amount of CO_2 were produced concurrently with acetaldehyde at both temperatures, and C_2H_4 and H_2O were produced at 610 K. The C_2H_5OH TPD results for the 12 wt % sample (Figure 8c) are similar to those of the 1 wt % sample with the exception that the peaks are somewhat larger and only the high-temperature CO peak is observed. More significant changes occurred for the 20 wt % sample (Figure 8d). For this sample only, the high-temperature

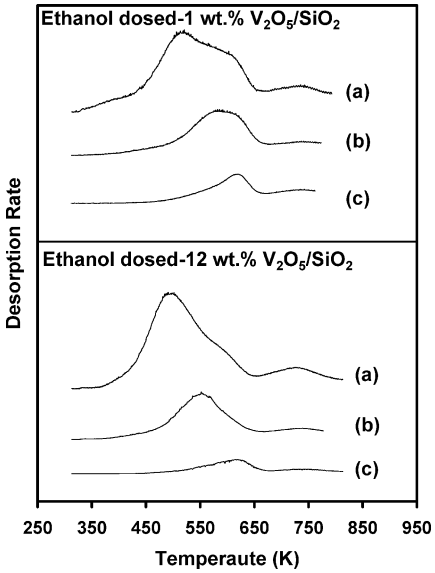

Figure 9. CH_3CHO desorption spectra obtained from CH_3CH_2OH-dosed, 1 and 12 wt % V_2O_5/SiO_2 following various sample pretreatments: (a) freshly prepared sample, (b) subsequent TPD run with the sample used in (a), and (c) after reoxidation of the sample used in (b) in 1 Torr O_2 at 775 K.

CH_3CHO peak is present and the CO and C_2H_4 peaks near 600 K are substantially larger than those from the lower vanadia coverage samples. Because this sample contains crystalline vanadia, these results indicate that the CH_3CHO, C_2H_4, CO, and CO_2 produced near 610 K are due to reaction on V_2O_5 crystallites. The lower temperature CH_3CHO peak that is present in the TPD spectra from the 1 and 12 wt % samples can, therefore, be attributed to reaction on the dispersed vanadia monolayer.

Figure 9 displays the acetaldehyde desorption curves obtained during C_2H_5OH TPD runs for both the 1 and the 12 wt % samples as a function of the sample pretreatment conditions. In this figure, curve a corresponds to a freshly prepared sample, curve b was obtained in the subsequent C_2H_5OH TPD run, and curve c was obtained after oxidizing the sample used in (b) in 1 Torr O_2 at 775 K. Note that for both vanadia weight loadings the low-temperature CH_3CHO peak is nearly absent in the second TPD run. This result is similar to what has been reported previously in TPD studies of the reaction of CH_3OH on V_2O_5/TiO_2 and V_2O_5/CeO_2.[25,30] As noted above, in these previous studies it was found that the oxidation state of the vanadium cations affected the temperature at which formaldehyde was produced via dehydrogenation of an adsorbed methoxide with a decrease in the oxidation state causing an increase in the CH_2O peak temperature. Thus, the disappearance of the low-temperature CH_3CHO peak in the second C_2H_5OH TPD run may be due to partial reduction of the vanadia layer. Note, however, that reoxidation of the V_2O_5/SiO_2 catalysts did not result in the reappearance of the low-temperature acetaldehyde peaks (see curve c in Figure 9). In fact, oxidation of the catalyst produced a further increase in the acetaldehyde desorption temperature and a nearly 3-fold increase in the area of the CO and C_2H_4 peaks at 600 K (not shown in the figure). The TPD spectra for reoxidized samples were similar to those obtained form the 20 wt % vanadia sample that contained primarily vanadia crystallites. This result indicates that the oxidation treatment induced agglomeration of the dispersed vanadia into small crystallites.

Changes in the structure of the vanadia induced by exposure to alcohols and/or heating were characterized using XRD and Raman spectroscopy. Figure 10 exhibits XRD patterns for a 12 wt % V_2O_5/SiO_2 sample that were obtained for pretreatment conditions similar to those used in the TPD experiments, that is, a freshly prepared sample (curve a), the same sample following an ethanol TPD run (curve b), and after oxidation of the sample used in (b) in 1 Torr of O_2 at 775 K (curve c). As described above, the XRD pattern of the fresh sample contained features which are indicative of V_2O_5 crystallites. The peaks due to the V_2O_5 crystallites are not present in the diffraction pattern obtained form the sample subjected to an ethanol TPD run, but are replaced by peaks at 27.7° and 37.1° which are indicative of VO_2[53] and demonstrate partial reduction of the vanadia layer. The XRD pattern of the reoxidized sample was similar to that of the fresh sample and contained peaks indicative of V_2O_5 crystallites. The peaks were slightly more intense in the reoxidized sample as compared to the fresh sample, again suggesting additional agglomeration of the dispersed vanadia into vanadia crystallites.

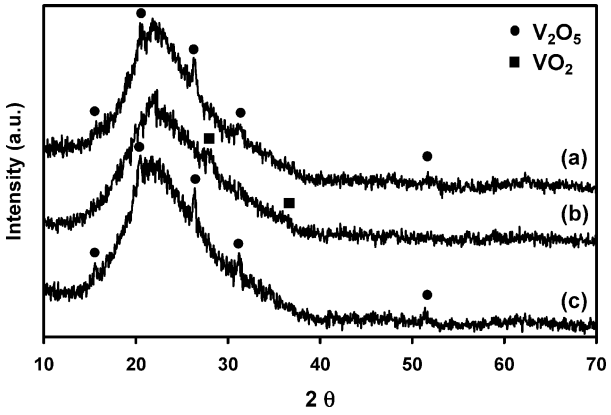

Figure 10. X-ray diffraction patterns of 12 wt % V_2O_5/SiO_2: (a) freshly prepared sample, (b) subsequent TPD run with the sample used in (a), and (c) after reoxidation of the sample used in (b) in 1 Torr O_2 at 775 K.

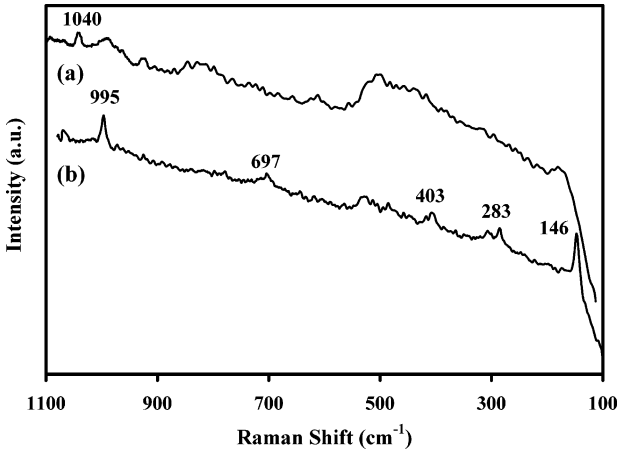

Figure 11. Raman spectra of 1 wt % V_2O_5/SiO_2: (a) freshly prepared sample, and (b) annealed in a vacuum at 775 K.

Raman spectra were collected for samples that had been exposed to methanol or ethanol and heated and for samples that had been heated in a vacuum. The results were similar for both pretreatments, so only the spectra for the samples heated in a vacuum will be discussed. These spectra are presented in Figure 11. Curve a in this figure corresponds to a freshly prepared 1 wt % V_2O_5/SiO_2 sample, and curve b is from the same sample after annealing in a vacuum at 775 K. As described above, the spectrum for the fresh sample contains a peak at 1040 cm^{-1} due to the V═O stretching mode of isolated VO_4 species. The

remaining peaks are due to the silica support. Annealing the sample at 775 K resulted in the disappearance of the peak at 1040 cm^{-1} due to isolated VO_4 species, and new features have emerged at 995, 697, 403, 283, and 146 cm^{-1}. These later peaks can be assigned to crystalline V_2O_5.[14−16] This result indicates that annealing at 775 K in a vacuum is sufficient to induce agglomeration of the vanadia layer.

Discussion

The TPD peak temperatures for the production of CH_2O via the dehydrogenation of adsorbed methoxide intermediates obtained in this study for dispersed vanadia on SiO_2 are substantially higher than those reported previously for V_2O_5/CeO_2 and V_2O_5/TiO_2. The DRIFTS results indicate that the CH_2O peaks in the TPD spectra are due to the reaction of methoxide intermediates on the vanadia and not the silica. As noted above, on the basis of these results, it is tempting to conclude from this result that the activation energy for the dehydrogenation of methoxide species on dispersed vanadia on SiO_2 is significantly higher than that on TiO_2 and CeO_2. The similarity between the TPD results obtained for the 1 and 12 wt % samples and that obtained for the 20 wt % sample, which contained vanadia crystallites, as well as the Raman and XRD results, however, indicates that for all three vanadia weight loadings the production of CH_2O at temperatures above 650 K can be attributed to reaction of methoxide intermediates on V_2O_5 crystallites. Because both XRD and Raman showed that the 1 and 12 wt % samples contained dispersed vanadia prior to exposure to methanol, it appears that agglomeration of the dispersed vanadia into crystallites occurred during the TPD experiment. This is in contrast to V_2O_5/CeO_2 and V_2O_5/TiO_5 for which multiple methanol or ethanol TPD experiments in which the sample is heated to 800 K can be performed without inducing agglomeration of the dispersed vanadia. Thus, the results of the present study indicate that there is relatively weak bonding between dispersed VO_4 species and a silica support. This conclusion is consistent with previous in situ Raman studies.[16]

Unfortunately, the agglomeration of the vanadia layer while heating CH_3OH-dosed V_2O_5/SiO_2 samples precludes the use of TPD to measure the activation energy for the dehydrogenation of adsorbed methoxide intermediates on dispersed vanadia on SiO_2. Insight into the activation energy for the dehydrogenation of alkoxides on V_2O_5/SiO_2 can be obtained, however, from the ethanol TPD results. While some agglomeration of the vanadia layer occurs during TPD with C_2H_5OH-dosed samples, peaks indicative of the dehydrogenation of ethoxide intermediates adsorbed on dispersed vanadia are still readily apparent in the TPD spectra. For example, in the ethanol TPD spectra for the 12 wt % sample, the CH_3CHO peak centered at 475 K can be attributed to reaction on dispersed VO_4. This peak shifts to higher temperature as the VO_4 layer becomes partially reduced and appears at 625 K upon agglomeration of the vanadia into crystallites. It is useful to compare this result to what was obtained in previous TPD studies of the reaction of ethanol on V_2O_5/CeO_2 and V_2O_5/TiO_2.[54] In those studies, it was found that for fully oxidized 6 wt % V_2O_5/CeO_2 and 7 wt % V_2O_5/TiO_2 acetaldehyde is produced during ethanol TPD at 455 and 450 K, respectively. Using these peak temperatures and assuming a preexponential factor of 10^{13} s^{-1}, analysis of the TPD data gives activation energies for the dehydrogenation of the ethoxide of 127, 126, and 132 kJ/mol for V_2O_5/CeO_2, V_2O_5/TiO_2, and V_2O_5/SiO_2, respectively. While this result indicates that the activation energy for dehydrogenation of the alkoxide, which is generally believed to be the rate-limiting step for the selective oxidation of alcohols, may be slightly higher on V_2O_5/SiO_2 as compared to those on V_2O_5/CeO_2 and V_2O_5/TiO_2, the difference is not nearly large enough to account for the large discrepancy in the TOF frequencies for the selective oxidation of alcohols on these catalysts. As noted in the Introduction, the TOF for the oxidation of methanol to formaldehyde on V_2O_5/SiO_2 has been reported to be over 2 orders of magnitude less than that on V_2O_5/CeO_2 and V_2O_5/TiO_2.[22] While this study does not provide a definitive explanation for the large difference in the activity of supported vanadia catalysts with changes in the support, it does suggest that, in the case of vanadia on silica, agglomeration of the vanadia into small crystallites may be partially responsible for its low activity.

Note that the data for the 20 wt % V_2O_5/SiO_2 sample shows that small supported crystallites still exhibit some activity for the selective oxidation of the alcohols, albeit with a much higher activation energy than that for the dispersed vanadia. The supported small crystallites also exhibit significantly higher activity than bulk V_2O_5. This result may be due to a higher concentration of defects, such as oxygen vacancies, that act as adsorption sites on the small supported crystallites as compared to bulk vanadia.

It is interesting that peaks indicative of the reaction of alkoxide species on dispersed vanadia are present in the data for ethanol and not methanol. Assuming that agglomeration of the vanadia is thermally induced, one possible explanation for this is a difference in the activation energy for dehydrogenation of a methoxide relative to an ethoxide. Our previous TPD studies of the reaction alcohols on V_2O_5/CeO_2 and TiO_2/TiO_2 have shown that the peak temperature for the production of the aldehyde from an ethoxide is 65−85 K lower than that from a methoxide. Thus, it is possible that agglomeration of the vanadia layer starts to occur at temperatures only slightly higher than the acetaldehyde peak temperature of 475 K, which is lower than the expected formaldehyde peak temperature from dispersed vanadia. While this purely thermal effect may partially explain the differences in the TPD results for methanol and ethanol, the TPD data in Figures 5 and 9 suggest that agglomeration of the dispersed vanadia still occurred more readily on the CH_3OH-dosed samples. Thus, it is possible that the presence of methoxide species adsorbed on the dispersed vanadia increases their mobility and helps to facilitate agglomeration. Note that a similar conclusion has been reported previously for the effect of methoxide species on the surface mobility of dispersed molybdena on silica.[48,55]

Conclusions

Temperature-programmed desorption was used to characterize the reactivity of vanadia supported on silica for the oxidation of both methanol and ethanol. Methanol TPD results for 1, 12, and 20 wt % V_2O_5/SiO_2 samples were surprisingly similar, with formaldehyde being produced at temperatures near 675 K. This result along with Raman spectra and X-ray diffraction data indicates that the dispersed vanadia underwent agglomeration during a methanol TPD run. This precluded the use of TPD to measure the activation energy for dehydrogenation of adsorbed methoxide intermediates on dispersed vanadia supported on silica. In contrast to the methanol TPD results, the TPD spectra obtained from ethanol-dosed samples exhibited a stronger dependence on the vanadia loading and pretreatment conditions. The trends in the ethanol TPD spectra were also similar to those reported previously for the reaction of methanol on V_2O_5/CeO_2 and V_2O_5/TiO_2. These results indicate that agglomeration of the

vanadia layer during TPD run was less severe for ethanol-dosed samples as compared to methanol dosed-samples. On the basis of the CH_3CHO TPD peak temperature, the activation energy for the dehydrogenation of adsorbed ethoxide intermediates to produce acetaldehyde was estimated to be 132 kJ/mol. The results of this study further demonstrate that vanadia interacts only weakly with a silica support and suggest that adsorbed methoxide species help facilitate agglomeration of dispersed vanadia on silica.

Acknowledgment. We gratefully acknowledge the financial support of the National Science Foundation (Grant No. CTS-01-39613) and the Laboratory for Research on the Structure of Matter at the University of Pennsylvania for the use of its facilities.

References and Notes

(1) Bond, G. C.; Tahir, S. F. *Appl. Catal., A* **1991**, *71*, 1.
(2) Satterfield, C. N. *Heterogeneous Catalysis in Industrial Practice*; Krieger Pub Co.: Malabar, FL, 1996.
(3) Deo, G.; Wachs, I. E. *J. Catal.* **1994**, *146*, 323.
(4) Hanuza, J.; Jezowska-Trzebiatowska, B.; Oganowski, W. *J. Mol. Catal.* **1985**, *29*, 109.
(5) Busca, G. *Mater. Chem. Phys.* **1988**, *19*, 157.
(6) Went, G. T.; Oyama, S. T.; Bell, A. T. *J. Phys. Chem.* **1990**, *94*, 4240.
(7) Deo, G.; Wachs, I. E.; Haber, J. *Crit. Rev. Surf. Chem.* **1994**, *4*, 141.
(8) Wachs, I. E.; Weckhuysen, B. M. *Appl. Catal., A* **1997**, *157*, 67.
(9) Jrusta, S.; Cornaglia, L. M.; Miro, E. E.; Lombardo, E. A. *J. Catal.* **1995**, *156*, 167.
(10) Das, N.; Hellmut, E.; Hu, H.; Wachs, I. E.; Walzer, J. F.; Feher, F. J. *J. Phys. Chem.* **1993**, *97*, 8240.
(11) Baiker, A.; Dollenmeier, P.; Glinski, M.; Reller, A.; Sharma, V. K. *J. Catal.* **1988**, *111*, 273.
(12) Wang, C.-B.; Deo, G.; Wachs, I. E. *J. Catal.* **1998**, *178*, 640.
(13) Gao, X.; Bare, S. R.; Weckhuysen, B. M.; Wachs, I. E. *J. Phys. Chem. B* **1998**, *102*, 10842.
(14) Xie, S.; Iglesia, E.; Bell, A. T. *Langmuir* **2000**, *16*, 7162.
(15) Jehng, J.-M.; Hu, H.; Gao, X.; Wachs, I. E. *Catal. Today* **1996**, *28*, 335.
(16) Owens, L.; Kung, H. H. *J. Catal.* **1993**, *144*.
(17) Keranen, J.; Guimon, C.; Iiskola, E.; Auroux, A.; Niinisto, L. *J. Phys. Chem. B* **2003**, *107*, 10773.
(18) Wang, C.-B.; Cai, Y.; Wachs, I. E. *Langmuir* **1999**, *15*, 1223.
(19) Khodakov, A.; Olthof, B.; Bell, A. T.; Iglesia, E. *J. Catal.* **1999**, *181*, 205.
(20) Koranne, M. M.; Goodwin, J. G., Jr.; Marcelin, G. *J. Catal.* **1994**, *148*, 388.
(21) Eckert, H.; Wachs, I. E. *J. Phys. Chem.* **1989**, *93*, 6796.
(22) Burcham, L. J.; Briand, L. E.; Wachs, I. E. *Langmuir* **2001**, *17*, 6164.
(23) Wong, G. S.; Kragten, D. D.; Vohs, J. M. *Surf. Sci.* **2000**, *452*, L293.
(24) Wong, G. S.; Kragten, D. D.; Vohs, J. M. *J. Phys. Chem. B* **2001**, *105*, 1366.
(25) Feng, T.; Vohs, J. M. *J. Catal.* **2002**, *208*, 301.
(26) Wong, G. S.; Concepcion, M. R.; Vohs, J. M. *J. Phys. Chem. B* **2002**, *106*, 6451.
(27) Wong, G. S.; Vohs, J. M. *Surf. Sci.* **2002**, *498*, 266.
(28) Wong, G. S.; Concepcion, M. R.; Vohs, J. M. *Surf. Sci.* **2003**, *526*, 211.
(29) Vohs, J. M.; Feng, T.; Wong, G. S. *Catal. Today* **2003**, *85*, 303.
(30) Feng, T.; Vohs, J. M. *J. Catal.* **2004**, *221*, 619.
(31) Holstein, W. L.; Machiels, C. J. *J. Catal.* **1996**, *162*, 118.
(32) Burcham, L. J.; Wachs, I. E. *Catal. Today* **1999**, *49*, 467.
(33) Wachs, I. E.; Deo, G.; Juskelis, M. V.; Weckhuysen, B. M. *Stud. Surf. Sci. Catal.* **1997**, *109*, 305.
(34) Feng, T.; Barker, G. A.; Vohs, J. M. *Langmuir* **2003**, *19*, 1268.
(35) Inumaru, K.; Misono, M.; Okuhara, T. *Appl. Catal., A* **1997**, *149*, 133.
(36) Jonson, B.; Rebenstorf, B.; Larsson, R.; Andersson, S. L. T. *J. Chem. Soc., Faraday Trans.* **1988**, *84*, 1897.
(37) Anpo, M.; Sunamoto, M.; Che, M. *J. Phys. Chem.* **1989**, *93*, 1187.
(38) Arena, F.; Frusteri, F.; Martra, G.; Coluccia, S.; Parmaliana, A. *J. Chem. Soc., Faraday Trans.* **1997**, *93*, 3849.
(39) Hazenkamp, M. F.; Blasse, G. *J. Phys. Chem.* **1992**, *96*, 3442.
(40) Wachs, I. E. *Catal. Today* **1996**, *27*, 437.
(41) Jehng, J.-M.; Deo, G.; Weckhuysen, B. M.; Wachs, I. E. *J. Mol. Catal.* **1996**, *110*, 41.
(42) Morrow, B. A.; McFarlan, A. J. *J. Non-Cryst. Solids* **1990**, *120*, 61.
(43) Brinker, C. J.; Kirkpatrick, R. J.; Tallant, D. R.; Bunker, B. C.; Montez, B. *J. Non-Cryst. Solids* **1988**, *99*, 418.
(44) Wovchko, E. A.; Camp, J. C.; Glass, J. A., Jr.; Yates, J. T. *Langmuir* **1995**, *11*, 2592.
(45) Morrow, B. A. *J. Chem. Soc., Faraday Trans. 1* **1974**, *70*, 1527.
(46) Forester, T. R.; Howe, R. F. *J. Am. Chem. Soc.* **1987**, *109*, 5076.
(47) Rasko, J.; Bontovics, J.; Solymosi, F. *J. Catal.* **1994**, *146*, 22.
(48) Seman, M.; Kondo, J. N.; Domen, K.; Radhakrishnan, R.; Oyama, S. T. *J. Phys. Chem. B* **2002**, *106*, 12965.
(49) Clarke, D. B.; Lee, D.-K.; Sandoval, M. J.; Bell, A. T. *J. Catal.* **1994**, *150*, 81.
(50) Morterra, C.; Magnacca, G.; Bolis, V. *Catal. Today* **2001**, *70*, 43.
(51) Novak, E.; Hancz, A.; Erdohelyi, A. *Radiat. Phys. Chem.* **2003**, *66*, 27.
(52) Busca, G.; Elmi, A. S.; Forzatti, P. *J. Phys. Chem.* **1987**, *91*, 5263.
(53) Powder Diffraction File #44-0253, International Center for Diffraction Data.
(54) Feng, T.; Vohs, J. M. *J. Phys. Chem. B* **2004**, *108*, 5647.
(55) Banares, M. A.; Hu, H.; Wachs, I. E. *J. Catal.* **1994**, *150*, 407.